First Experimental Study of Photon Polarization in Radiative B_s^0 Decays

R. Aaij *et al.*[*]
(LHCb Collaboration)

(Received 10 September 2016; published 9 January 2017; corrected 28 February 2017)

The polarization of photons produced in radiative B_s^0 decays is studied for the first time. The data are recorded by the LHCb experiment in pp collisions corresponding to an integrated luminosity of 3 fb^{-1} at center-of-mass energies of 7 and 8 TeV. A time-dependent analysis of the $B_s^0 \to \phi\gamma$ decay rate is conducted to determine the parameter $\mathcal{A}^\Delta$, which is related to the ratio of right- over left-handed photon polarization amplitudes in $b \to s\gamma$ transitions. A value of $\mathcal{A}^\Delta = -0.98^{+0.46\,+0.23}_{-0.52\,-0.20}$ is measured. This result is consistent with the standard model prediction within 2 standard deviations.

DOI: 10.1103/PhysRevLett.118.021801

In the standard model (SM), photons emitted in $b \to s\gamma$ transitions are produced predominantly with a left-handed polarization, with a small right-handed component proportional to the ratio of the quark masses, m_s/m_b. In many extensions of the SM, the right-handed component can be enhanced, leading to observable effects in mixing-induced CP asymmetries and time-dependent decay rates of radiative B^0 and B_s^0 decays [1,2]. Measurements of the time-dependent CP asymmetries in radiative heavy meson decays have been performed by the *BABAR* and Belle Collaborations in the B^0 system only [3]. The production of polarized photons in $b \to s\gamma$ transitions was observed for the first time at LHCb by studying the up-down asymmetry in $B^+ \to K^+\pi^-\pi^+\gamma$ decays [4] (charge conjugation is implied throughout the text). In addition, angular observables in the $B^0 \to K^{*0}e^+e^-$ channel for dielectron invariant masses of less than 1 GeV/c^2 that are sensitive to the polarization of the virtual photon have also been measured at LHCb [5]. All of these measurements are found to be in agreement with the SM predictions.

This Letter reports the first experimental study of the photon polarization in radiative B_s^0 decays, determined from the time dependence of the rate of $B_s^0 \to \phi\gamma$ decays. The rate at which B_s^0 or $\bar{B}_s^0$ mesons decay to a common final state that contains a photon, such as $\phi\gamma$, depends on the decay time t and is proportional to

$$e^{-\Gamma_s t}\{\cosh(\Delta\Gamma_s t/2) - \mathcal{A}^\Delta \sinh(\Delta\Gamma_s t/2) + \zeta\mathcal{C}\cos(\Delta m_s t) - \zeta\mathcal{S}\sin(\Delta m_s t)\}, \quad (1)$$

where $\Delta\Gamma_s$ and Δm_s are the width and mass differences between the light and heavy B_s^0 mass eigenstates, Γ_s is the mean decay width, and ζ takes the value $+1$ for an initial B_s^0 state and -1 for $\bar{B}_s^0$. The coefficients $\mathcal{C}$, $\mathcal{S}$, and $\mathcal{A}^\Delta$ are functions of the left- and right-handed photon polarization amplitudes [2]. The terms $\mathcal{C}$ and $\mathcal{S}$ can be measured only if the initial flavor is known: for an approximately equal mixture of B_s^0 and $\bar{B}_s^0$ mesons, as used in this analysis, these terms cancel and the photon polarization affects only the parameter $\mathcal{A}^\Delta$. This approach has the advantage that there is no need to determine the flavor of the B_s^0 candidates at production, which would considerably reduce the effective size of the data sample. Compared to the B^0 system, the B_s^0 is unique in that the sizable width difference allows $\mathcal{A}^\Delta$ to be measured. In the SM it can be parametrized as $\mathcal{A}^\Delta = \sin(2\psi)$, where $\tan\psi \equiv |A(\bar{B}_s^0 \to \phi\gamma_R)|/|A(\bar{B}_s^0 \to \phi\gamma_L)|$ is the ratio of right- and left-handed photon amplitudes. The SM prediction is $\mathcal{A}^\Delta_{\rm SM} = 0.047^{+0.029}_{-0.025}$ [2].

This analysis is based on a data sample corresponding to 3 fb^{-1} of integrated luminosity, collected by the LHCb experiment in pp collisions at center-of-mass energies of 7 and 8 TeV in 2011 and 2012, respectively. The LHCb detector is a single-arm forward spectrometer covering the pseudorapidity range $2 < \eta < 5$, described in detail in Refs. [6,7]. Different types of charged hadrons are distinguished using information from two ring-imaging Cherenkov detectors. The online event selection is performed by a trigger, which consists of a hardware stage, based on information from the calorimeter and muon systems, followed by a software stage, which applies a full event reconstruction. Two trigger selections are defined with different photon and track momentum thresholds, depending on whether the hardware stage triggered on one of the tracks or on the photon. Samples of simulated events, produced with the software described in Refs. [8–13], are used to characterize signal and background contributions.

The decay mode $B^0 \to K^{*0}\gamma$, with $K^{*0} \to K^+\pi^-$, is used as a control channel. Since it is a flavor-specific decay, its decay-time distribution is not sensitive to the photon polarization. Throughout this Letter, K^{*0} denotes

[*]Full author list given at the end of the article.

$K^*(892)^0$. Candidate $B_s^0 \to \phi\gamma$ and $B^0 \to K^{*0}\gamma$ decays are reconstructed from a photon, and two oppositely charged tracks: two kaons to reconstruct $\phi \to K^+K^-$ decays and a kaon and a pion to reconstruct $K^{*0} \to K^+\pi^-$ decays. The selection is designed to maximize the expected significance of the signal yield. Photons are reconstructed from energy deposits in the electromagnetic calorimeter and are required to have momentum transverse to the beam axis, p_T, larger than 3.0 or 4.2 GeV/c, depending on the trigger selection. Each charged particle is required to have a minimum p_T of 0.5 GeV/c and at least one of them must have p_T larger than 1.7 or 1.2 GeV/c, depending on the trigger selection. The tracks are required to be inconsistent with originating from a primary pp interaction vertex. The pion and kaon candidates are required to be identified by the particle identification system. The two tracks must meet at a common vertex and have an invariant mass within 15 MeV/c^2 of the known ϕ mass [14] for the signal mode, or within 100 MeV/c^2 of the known K^{*0} mass for the control mode. Each B_s^0 or B^0 candidate is required to have p_T larger than 3.0 GeV/c, and a reconstructed momentum vector consistent with originating from one and only one primary vertex. Background due to photons from π^0 decays is rejected by a dedicated algorithm [15]. In addition, the cosine of the helicity angle, defined as the angle between the positively charged hadron and the B meson in the rest frame of the ϕ or K^{*0} meson, is required to be less than 0.8.

A kinematic fit of the full decay chain is performed, imposing a constraint on the mass of the B candidate. Its decay time is determined from the fitted four-momentum and flight distance from the primary vertex. The mass constraint improves the decay-time resolution and also ensures that it is not correlated with the reconstructed mass for the signal. Only candidates with decay times between 0.3 and 10 ps are retained.

The B_s^0 and B^0 signal yields are obtained from separate extended unbinned maximum likelihood fits to the $\phi\gamma$ and $K^{*0}\gamma$ invariant mass distributions, shown in Fig. 1. The signal line shapes are described by modified Crystal Ball functions [16] with tails on both sides of the peak. The tail parameters are determined from simulation. Three background categories are considered: peaking, partially reconstructed, and combinatorial backgrounds. Peaking backgrounds are due to the misidentification of a final-state particle. All possible sources of misidentified tracks, as well as misidentification of a π^0 meson as a photon, are considered for the signal and control channels. Partially reconstructed backgrounds, in which one or more final-state particles are not reconstructed, are described with an ARGUS function [17] convolved with a Gaussian function to account for the mass resolution of the detector. The dominant contributions are decays with a missing pion or kaon, $B \to K\pi\pi^0X$, and $B^0 \to K^{*0}\eta$. All shape parameters for the peaking and partially reconstructed backgrounds are fixed from simulation. The ratios of the yields of peaking backgrounds to signal are fixed using previous measurements [14,18]. A first-order polynomial is used to describe the combinatorial background. The signal yields are 4072 ± 112 and $24\,808 \pm 321$ for the $B_s^0 \to \phi\gamma$ and $B^0 \to K^{*0}\gamma$ decays, where the uncertainties are statistical only.

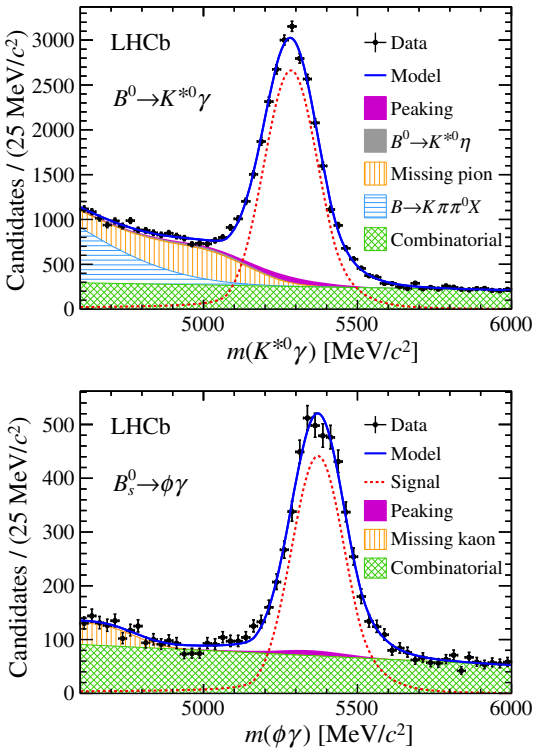

FIG. 1. Fits to the invariant mass distributions of the B^0 (top) and B_s^0 (bottom) candidates.

The mass fits are used to assign each candidate of the $B_s^0 \to \phi\gamma$ and $B^0 \to K^{*0}\gamma$ samples a signal weight to subtract the backgrounds [19]. An unbinned maximum likelihood fit of the weighted decay-time distributions [20] is then performed simultaneously on the $B_s^0 \to \phi\gamma$ and $B^0 \to K^{*0}\gamma$ samples. The signal probability density function (PDF) is defined from the product of the decay-time-dependent signal rate $\mathcal{P}(t)$ and the efficiency $\epsilon(t)$, convolved with the resolution.

For $B_s^0 \to \phi\gamma$, Eq. (1) reduces to

$$\mathcal{P}(t) \propto e^{-\Gamma_s t}\{\cosh(\Delta\Gamma_s t/2) - \mathcal{A}^{\Delta}\sinh(\Delta\Gamma_s t/2)\}, \qquad (2)$$

when summing over the initial B_s^0 and $\bar{B}_s^0$ states. The B_s^0 and $\bar{B}_s^0$ production rates are assumed to be equal, given that their measured asymmetries [21] are found to have a negligible effect on the measurement of $\mathcal{A}^{\Delta}$. For $B^0 \to K^{*0}\gamma$, the decay-time-dependent signal rate is a single exponential function, $\mathcal{P}(t) \propto e^{-t/\tau_{B^0}}$. The physics parameters τ_{B^0}, Γ_s, and $\Delta\Gamma_s$ are constrained to the averages from Ref. [3]: $\tau_{B^0} = 1.520 \pm 0.004$ ps, $\Gamma_s = 0.6643 \pm 0.0020$ ps^{-1}, and $\Delta\Gamma_s = 0.083 \pm 0.006$ ps^{-1}. The correlation

of −0.239 between the uncertainties on Γ_s and $\Delta\Gamma_s$ is taken into account.

To ensure that the simulation reproduces the decay-time resolution, additional control samples of $B_s^0 \to J/\psi\phi$ and $B^0 \to J/\psi K^{*0}$ decays are used, where the J/ψ meson is reconstructed from a pair of oppositely charged muons. Selections mimicking those of $B_s^0 \to \phi\gamma$ and $B^0 \to K^{*0}\gamma$, treating the J/ψ meson as a photon, are applied. The distributions of the difference in position between the reconstructed J/ψ and ϕ or K^{*0} vertices are measured in data and simulation and found to be in agreement. The decay-time-dependent resolution functions are then determined from the simulation. The decay-time resolution is small compared to the b-hadron lifetimes, and similar for $B_s^0 \to \phi\gamma$ and $B^0 \to K^{*0}\gamma$.

The decay-time-dependent efficiency is parametrized as

$$\epsilon(t) = e^{-\alpha t}\frac{[a(t-t_0)]^n}{1+[a(t-t_0)]^n} \quad \text{for } t \geq t_0, \tag{3}$$

where the parameters a and n describe the curvature of the efficiency function at low decay times, t_0 is the decay time below which the efficiency function is zero, and α describes the decrease of the efficiency at high decay times. Large simulated samples of $B_s^0 \to \phi\gamma$ or $B^0 \to K^{*0}\gamma$ decays are used to validate this parametrization. The signal PDF is found to describe the reconstructed decay-time distribution of selected simulated candidates over the full decay-time range. The $B_s^0 \to \phi\gamma$ and $B^0 \to K^{*0}\gamma$ decay-time-dependent efficiency parameters are found to be similar. In a simultaneous fit of both simulation samples, requiring the parameters a and n to be the same for both channels does not change the quality of the fit. To assess whether the simulation reproduces the decay-time-dependent efficiency, the $B^0 \to K^{*0}\gamma$ data sample alone is used to fit τ_{B^0}, fixing in this case all the efficiency parameters to those from the simulation. The fitted value of τ_{B^0} is 1.524 ± 0.013 ps, where the uncertainty is statistical only, in agreement with the world average value [3]. In the simultaneous fit to the data, the parameters a and n are required to be the same for both channels and fixed to their values in the simulation. For t_0 and α, a global offset, the same for both channels, is allowed between data and the simulation.

Pseudoexperiments are used to validate the overall fit procedure. For each pseudoexperiment, samples of $B_s^0 \to \phi\gamma$ and $B^0 \to K^{*0}\gamma$ candidates are generated, including both signal and background contributions. The expected yields are taken from the fit to the data, as is the signal mass shape. Background events are generated according to the mass and decay-time PDFs determined from fits to samples of events generated with the full LHCb simulation. For each pseudoexperiment, the mass fits to the $B_s^0 \to \phi\gamma$ and $B^0 \to K^{*0}\gamma$ samples are performed, followed by the decay-time fit to the background-subtracted samples. The procedure is tested in samples of pseudoexperiments generated with different values of $\mathcal{A}^\Delta$. No bias on the average fitted value of $\mathcal{A}^\Delta$ is observed. Statistical uncertainties are found to be underestimated by an amount that depends on $\mathcal{A}^\Delta$; the effect is 5.8% for the value seen in data and is accounted for in the results below.

The $B^0 \to K^{*0}\gamma$ and $B_s^0 \to \phi\gamma$ background-subtracted decay-time distributions and the corresponding fit projections, including the ones for the central value of the SM prediction for $\mathcal{A}^\Delta$, are shown in Fig. 2. The fitted value of $\mathcal{A}^\Delta$ is $-0.98^{+0.46}_{-0.52}$. The statistical uncertainty includes a contribution due to the uncertainties on the physics parameters τ_{B^0}, Γ_s, and $\Delta\Gamma_s$, which is estimated to account for $^{+0.10}_{-0.17}$.

In an alternative approach, $\mathcal{A}^\Delta$ is calculated from the ratio of the yields of $B_s^0 \to \phi\gamma$ and $B^0 \to K^{*0}\gamma$ in bins of decay time. Based on a study of pseudoexperiments, the binning scheme is designed to have the same number of events in each bin, thereby optimizing the overall

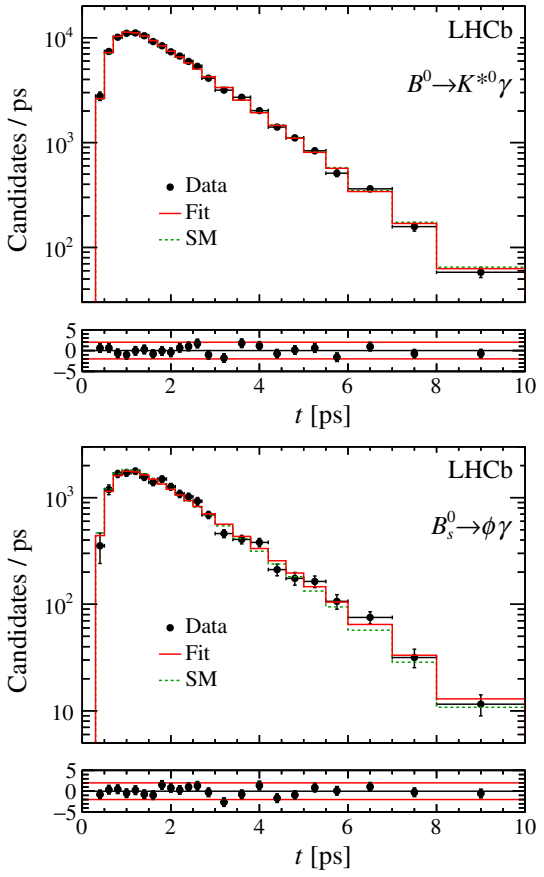

FIG. 2. Background-subtracted decay-time distributions for $B^0 \to K^{*0}\gamma$ (top) and $B_s^0 \to \phi\gamma$ (bottom) decays with the fit projections overlaid and normalized residuals shown below. The projections of a fit with $\mathcal{A}^\Delta$ fixed to the central value of the SM prediction [2] are also shown. For display purposes, the PDFs are shown as histograms, integrated across each decay-time interval.

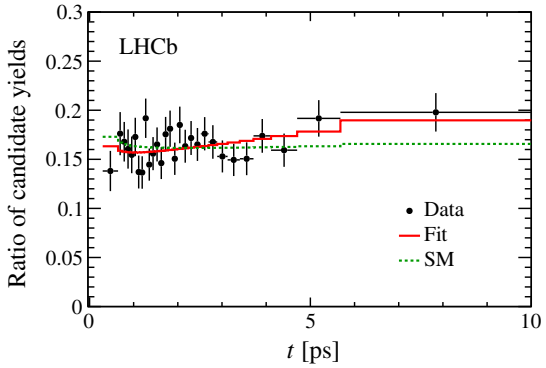

FIG. 3. Decay-time dependence of the ratio of the yields of $B_s^0 \to \phi\gamma$ and $B^0 \to K^{*0}\gamma$, with the fit overlaid. The expected distribution for the central value of the SM prediction [2] is also shown.

sensitivity to $\mathcal{A}^\Delta$. Decay-time-dependent efficiency and resolution effects are taken into account by calculating correction factors in each bin before fitting for $\mathcal{A}^\Delta$. Pseudoexperiments are used to validate this approach and to test its sensitivity, which is found to be equivalent to that of the baseline procedure. The fit to the data is shown in Fig. 3, along with the expected distribution for the central value of the SM prediction for $\mathcal{A}^\Delta$. The fitted value is $\mathcal{A}^\Delta = -0.85^{+0.43}_{-0.46}$. The statistical uncertainty is strongly correlated with that of the baseline approach; the difference between the two results is well within the range expected from pseudoexperiments.

The dominant systematic uncertainty comes from the background subtraction. It is evaluated to be $^{+0.19}_{-0.20}$ and includes contributions from potential correlations between the reconstructed mass and decay time for the backgrounds (± 0.15), uncertainties on the peaking background yields ($^{+0.02}_{-0.05}$), and the models used in the mass fit. The latter is assessed by the use of alternative models: an asymmetric Apollonios function [22] for the signal (± 0.03), an exponential for the combinatorial background (± 0.07), and several shape variations for the most relevant partially reconstructed backgrounds (± 0.10). The systematic uncertainty due to the limited size of the simulation samples used to assess the decay-time-dependent efficiency is $^{+0.13}_{-0.05}$. The uncertainties related to the decay-time resolution are negligible. The sum in quadrature of these systematic uncertainties is $^{+0.23}_{-0.20}$.

In summary, the polarization parameter $\mathcal{A}^\Delta$ is measured in the first time-dependent analysis of a radiative B_s^0 decay, using a data sample corresponding to an integrated luminosity of 3 fb^{-1} collected by the LHCb experiment. This parameter is related to the ratio of right- over left-handed photon polarization amplitudes in $b \to s\gamma$ transitions. More than 4000 $B_s^0 \to \phi\gamma$ decays are reconstructed. The decay-time-dependent efficiency is calibrated with a control sample of $B^0 \to K^{*0}\gamma$ decays that is 6 times larger. From an unbinned simultaneous fit to the $B_s^0 \to \phi\gamma$ and $B^0 \to K^{*0}\gamma$ data samples, a value of

$$\mathcal{A}^\Delta = -0.98^{+0.46\,+0.23}_{-0.52\,-0.20}$$

is measured, where the first uncertainty is statistical and the second systematic. The result is compatible with the SM expectation, $\mathcal{A}^\Delta_{\rm SM} = 0.047^{+0.029}_{-0.025}$ [2], within 2 standard deviations.

We express our gratitude to our colleagues in the CERN accelerator departments for the excellent performance of the LHC. We thank the technical and administrative staff at the LHCb institutes. We acknowledge support from CERN and from the national agencies: CAPES, CNPq, FAPERJ and FINEP (Brazil); NSFC (China); CNRS/IN2P3 (France); BMBF, DFG and MPG (Germany); INFN (Italy); FOM and NWO (Netherlands); MNiSW and NCN (Poland); MEN/IFA (Romania); MinES and FASO (Russia); MinECo (Spain); SNSF and SER (Switzerland); NASU (Ukraine); STFC (United Kingdom); NSF (USA). We acknowledge the computing resources that are provided by CERN, IN2P3 (France), KIT and DESY (Germany), INFN (Italy), SURF (Netherlands), PIC (Spain), GridPP (United Kingdom), RRCKI and Yandex LLC (Russia), CSCS (Switzerland), IFIN-HH (Romania), CBPF (Brazil), PL-GRID (Poland) and OSC (USA). We are indebted to the communities behind the multiple open source software packages on which we depend. Individual groups or members have received support from AvH Foundation (Germany), EPLANET, Marie Skłodowska-Curie Actions and ERC (European Union), Conseil Général de Haute-Savoie, Labex ENIGMASS and OCEVU, Région Auvergne (France), RFBR and Yandex LLC (Russia), GVA, XuntaGal and GENCAT (Spain), Herchel Smith Fund, The Royal Society, Royal Commission for the Exhibition of 1851 and the Leverhulme Trust (United Kingdom).

[1] D. Atwood, M. Gronau, and A. Soni, Mixing-Induced *CP* Asymmetries in Radiative *B* Decays in and Beyond the Standard Model, Phys. Rev. Lett. **79**, 185 (1997).
[2] F. Muheim, Y. Xie, and R. Zwicky, Exploiting the width difference in $B_s \to \phi\gamma$, Phys. Lett. B **664**, 174 (2008).
[3] Y. Amhis *et al.* (Heavy Flavor Averaging Group), Averages of *b*-hadron, *c*-hadron, and τ-lepton properties as of summer 2014, arXiv:1412.7515.
[4] R. Aaij *et al.* (LHCb Collaboration), Observation of Photon Polarization in the $b \to s\gamma$ Transition, Phys. Rev. Lett. **112**, 161801 (2014).
[5] R. Aaij *et al.* (LHCb Collaboration), Angular analysis of the $B^0 \to K^{*0}e^+e^-$ decay in the low-q^2 region, J. High Energy Phys. 04 (2015) 064.
[6] A. A. Alves Jr. *et al.* (LHCb Collaboration), The LHCb detector at the LHC, J. Instrum. **3**, S08005 (2008).

[7] R. Aaij *et al.* (LHCb Collaboration), LHCb detector performance, Int. J. Mod. Phys. A **30**, 1530022 (2015).
[8] T. Sjöstrand, S. Mrenna, and P. Skands, PYTHIA 6.4 physics and manual, J. High Energy Phys. 05 (2006) 026; A brief introduction to PYTHIA 8.1, Comput. Phys. Commun. **178**, 852 (2008).
[9] I. Belyaev *et al.*, Handling of the generation of primary events in Gauss, the LHCb simulation framework, J. Phys. Conf. Ser. **331**, 032047 (2011).
[10] D. J. Lange, The EvtGen particle decay simulation package, Nucl. Instrum. Methods Phys. Res., Sect. A **462**, 152 (2001).
[11] P. Golonka and Z. Was, PHOTOS Monte Carlo: A precision tool for QED corrections in Z and W decays, Eur. Phys. J. C **45**, 97 (2006).
[12] J. Allison *et al.* (Geant4 Collaboration), Geant4 developments and applications, IEEE Trans. Nucl. Sci. **53**, 270 (2006); S. Agostinelli *et al.* (Geant4 Collaboration), Geant4: A simulation toolkit, Nucl. Instrum. Methods Phys. Res., Sect. A **506**, 250 (2003).
[13] M. Clemencic, G. Corti, S. Easo, C. R. Jones, S. Miglioranzi, M. Pappagallo, and P. Robbe, The LHCb simulation application, Gauss: Design, evolution and experience, J. Phys. Conf. Ser. **331**, 032023 (2011).
[14] K. A. Olive *et al.* (Particle Data Group), Review of Particle Physics, Chin. Phys. C **38**, 090001 (2014).
[15] M. Calvo Gomez *et al.*, Report No. LHCb-PUB-2015-016.
[16] T. Skwarnicki, Ph.D. thesis, Institute of Nuclear Physics, Krakow, 1986, DESY-F31-86-02.
[17] H. Albrecht *et al.* (ARGUS Collaboration), Search for hadronic $b \to u$ decays, Phys. Lett. B **241**, 278 (1990).
[18] R. Aaij *et al.* (LHCb Collaboration), Measurement of the ratio of branching fractions $\mathcal{B}(B^0 \to K^{*0}\gamma)/\mathcal{B}(B_s^0 \to \phi\gamma)$ and the direct CP asymmetry in $B^0 \to K^{*0}\gamma$, Nucl. Phys. **B867**, 1 (2013).
[19] M. Pivk and F. R. Le Diberder, sPlot: A statistical tool to unfold data distributions, Nucl. Instrum. Methods Phys. Res., Sect. A **555**, 356 (2005).
[20] Y. Xie, sFit: a method for background subtraction in maximum likelihood fit, arXiv:0905.0724.
[21] R. Aaij *et al.* (LHCb Collaboration), Measurement of the $\bar{B}^0$–B^0 and $\bar{B}_s^0$–B_s^0 production asymmetries in pp collisions at $\sqrt{s} = 7$ TeV, Phys. Lett. B **739**, 218 (2014).
[22] D. Martínez Santos and F. Dupertuis, Mass distributions marginalized over per-event errors, Nucl. Instrum. Methods Phys. Res., Sect. A **764**, 150 (2014).

R. Aaij,[40] B. Adeva,[39] M. Adinolfi,[48] Z. Ajaltouni,[5] S. Akar,[6] J. Albrecht,[10] F. Alessio,[40] M. Alexander,[53] S. Ali,[43] G. Alkhazov,[31] P. Alvarez Cartelle,[55] A. A. Alves Jr,[59] S. Amato,[2] S. Amerio,[23] Y. Amhis,[7] L. An,[41] L. Anderlini,[18] G. Andreassi,[41] M. Andreotti,[17,g] J. E. Andrews,[60] R. B. Appleby,[56] F. Archilli,[43] P. d'Argent,[12] J. Arnau Romeu,[6] A. Artamonov,[37] M. Artuso,[61] E. Aslanides,[6] G. Auriemma,[26] M. Baalouch,[5] I. Babuschkin,[56] S. Bachmann,[12] J. J. Back,[50] A. Badalov,[38] C. Baesso,[62] S. Baker,[55] W. Baldini,[17] R. J. Barlow,[56] C. Barschel,[40] S. Barsuk,[7] W. Barter,[40] M. Baszczyk,[27] V. Batozskaya,[29] B. Batsukh,[61] V. Battista,[41] A. Bay,[41] L. Beaucourt,[4] J. Beddow,[53] F. Bedeschi,[24] I. Bediaga,[1] L. J. Bel,[43] V. Bellee,[41] N. Belloli,[21,i] K. Belous,[37] I. Belyaev,[32] E. Ben-Haim,[8] G. Bencivenni,[19] S. Benson,[43] J. Benton,[48] A. Berezhnoy,[33] R. Bernet,[42] A. Bertolin,[23] F. Betti,[15] M.-O. Bettler,[40] M. van Beuzekom,[43] Ia. Bezshyiko,[42] S. Bifani,[47] P. Billoir,[8] T. Bird,[56] A. Birnkraut,[10] A. Bitadze,[56] A. Bizzeti,[18,u] T. Blake,[50] F. Blanc,[41] J. Blouw,[11] S. Blusk,[61] V. Bocci,[26] T. Boettcher,[58] A. Bondar,[36,w] N. Bondar,[31,40] W. Bonivento,[16] A. Borgheresi,[21,i] S. Borghi,[56] M. Borisyak,[35] M. Borsato,[39] F. Bossu,[7] M. Boubdir,[9] T. J. V. Bowcock,[54] E. Bowen,[42] C. Bozzi,[17,40] S. Braun,[12] M. Britsch,[12] T. Britton,[61] J. Brodzicka,[56] E. Buchanan,[48] C. Burr,[56] A. Bursche,[2] J. Buytaert,[40] S. Cadeddu,[16] R. Calabrese,[17,g] M. Calvi,[21,i] M. Calvo Gomez,[38,m] A. Camboni,[38] P. Campana,[19] D. Campora Perez,[40] D. H. Campora Perez,[40] L. Capriotti,[56] A. Carbone,[15,e] G. Carboni,[25,j] R. Cardinale,[20,h] A. Cardini,[16] P. Carniti,[21,i] L. Carson,[52] K. Carvalho Akiba,[2] G. Casse,[54] L. Cassina,[21,i] L. Castillo Garcia,[41] M. Cattaneo,[40] Ch. Cauet,[10] G. Cavallero,[20] R. Cenci,[24,t] M. Charles,[8] Ph. Charpentier,[40] G. Chatzikonstantinidis,[47] M. Chefdeville,[4] S. Chen,[56] S.-F. Cheung,[57] V. Chobanova,[39] M. Chrzaszcz,[42,27] X. Cid Vidal,[39] G. Ciezarek,[43] P. E. L. Clarke,[52] M. Clemencic,[40] H. V. Cliff,[49] J. Closier,[40] V. Coco,[59] J. Cogan,[6] E. Cogneras,[5] V. Cogoni,[16,40,f] L. Cojocariu,[30] P. Collins,[40] A. Comerma-Montells,[12] A. Contu,[40] A. Cook,[48] G. Coombs,[40] S. Coquereau,[38] G. Corti,[40] M. Corvo,[17,g] C. M. Costa Sobral,[50] B. Couturier,[40] G. A. Cowan,[52] D. C. Craik,[52] A. Crocombe,[50] M. Cruz Torres,[62] S. Cunliffe,[55] R. Currie,[55] C. D'Ambrosio,[40] F. Da Cunha Marinho,[2] E. Dall'Occo,[43] J. Dalseno,[48] P. N. Y. David,[43] A. Davis,[59] O. De Aguiar Francisco,[2] K. De Bruyn,[6] S. De Capua,[56] M. De Cian,[12] J. M. De Miranda,[1] L. De Paula,[2] M. De Serio,[14,d] P. De Simone,[19] C. T. Dean,[53] D. Decamp,[4] M. Deckenhoff,[10] L. Del Buono,[8] M. Demmer,[10] D. Derkach,[35] O. Deschamps,[5] F. Dettori,[40] B. Dey,[22] A. Di Canto,[40] H. Dijkstra,[40] F. Dordei,[40] M. Dorigo,[41] A. Dosil Suárez,[39] A. Dovbnya,[45] K. Dreimanis,[54] L. Dufour,[43] G. Dujany,[56] K. Dungs,[40] P. Durante,[40] R. Dzhelyadin,[37] A. Dziurda,[40] A. Dzyuba,[31] N. Déléage,[4] S. Easo,[51] M. Ebert,[52] U. Egede,[55] V. Egorychev,[32] S. Eidelman,[36,w] S. Eisenhardt,[52] U. Eitschberger,[10] R. Ekelhof,[10] L. Eklund,[53] Ch. Elsasser,[42] S. Ely,[61] S. Esen,[12] H. M. Evans,[49] T. Evans,[57] A. Falabella,[15] N. Farley,[47] S. Farry,[54] R. Fay,[54] D. Fazzini,[21,i] D. Ferguson,[52] V. Fernandez Albor,[39] A. Fernandez Prieto,[39] F. Ferrari,[15,40]

F. Ferreira Rodrigues,[1] M. Ferro-Luzzi,[40] S. Filippov,[34] R. A. Fini,[14] M. Fiore,[17,g] M. Fiorini,[17,g] M. Firlej,[28] C. Fitzpatrick,[41] T. Fiutowski,[28] F. Fleuret,[7,b] K. Fohl,[40] M. Fontana,[16,40] F. Fontanelli,[20,h] D. C. Forshaw,[61] R. Forty,[40] V. Franco Lima,[54] M. Frank,[40] C. Frei,[40] J. Fu,[22,q] E. Furfaro,[25,j] C. Färber,[40] A. Gallas Torreira,[39] D. Galli,[15,e] S. Gallorini,[23] S. Gambetta,[52] M. Gandelman,[2] P. Gandini,[57] Y. Gao,[3] L. M. Garcia Martin,[68] J. García Pardiñas,[39] J. Garra Tico,[49] L. Garrido,[38] P. J. Garsed,[49] D. Gascon,[38] C. Gaspar,[40] L. Gavardi,[10] G. Gazzoni,[5] D. Gerick,[12] E. Gersabeck,[12] M. Gersabeck,[56] T. Gershon,[50] Ph. Ghez,[4] S. Gianì,[41] V. Gibson,[49] O. G. Girard,[41] L. Giubega,[30] K. Gizdov,[52] V. V. Gligorov,[8] D. Golubkov,[32] A. Golutvin,[55,40] A. Gomes,[1,a] I. V. Gorelov,[33] C. Gotti,[21,i] M. Grabalosa Gándara,[5] R. Graciani Diaz,[38] L. A. Granado Cardoso,[40] E. Graugés,[38] E. Graverini,[42] G. Graziani,[18] A. Grecu,[30] P. Griffith,[47] L. Grillo,[21,40,i] B. R. Gruberg Cazon,[57] O. Grünberg,[66] E. Gushchin,[34] Yu. Guz,[37] T. Gys,[40] C. Göbel,[62] T. Hadavizadeh,[57] C. Hadjivasiliou,[5] G. Haefeli,[41] C. Haen,[40] S. C. Haines,[49] S. Hall,[55] B. Hamilton,[60] X. Han,[12] S. Hansmann-Menzemer,[12] N. Harnew,[57] S. T. Harnew,[48] J. Harrison,[56] M. Hatch,[40] J. He,[63] T. Head,[41] A. Heister,[9] K. Hennessy,[54] P. Henrard,[5] L. Henry,[8] J. A. Hernando Morata,[39] E. van Herwijnen,[40] M. Heß,[66] A. Hicheur,[2] D. Hill,[57] C. Hombach,[56] H. Hopchev,[41] W. Hulsbergen,[43] T. Humair,[55] M. Hushchyn,[35] N. Hussain,[57] D. Hutchcroft,[54] M. Idzik,[28] P. Ilten,[58] R. Jacobsson,[40] A. Jaeger,[12] J. Jalocha,[57] E. Jans,[43] A. Jawahery,[60] F. Jiang,[3] M. John,[57] D. Johnson,[40] C. R. Jones,[49] C. Joram,[40] B. Jost,[40] N. Jurik,[61] S. Kandybei,[45] W. Kanso,[6] M. Karacson,[40] J. M. Kariuki,[48] S. Karodia,[53] M. Kecke,[12] M. Kelsey,[61] I. R. Kenyon,[47] M. Kenzie,[49] T. Ketel,[44] E. Khairullin,[35] B. Khanji,[21,40,i] C. Khurewathanakul,[41] T. Kirn,[9] S. Klaver,[56] K. Klimaszewski,[29] S. Koliiev,[46] M. Kolpin,[12] I. Komarov,[41] R. F. Koopman,[44] P. Koppenburg,[43] A. Kosmyntseva,[32] A. Kozachuk,[33] M. Kozeiha,[5] L. Kravchuk,[34] K. Kreplin,[12] M. Kreps,[50] P. Krokovny,[36,w] F. Kruse,[10] W. Krzemien,[29] W. Kucewicz,[27,l] M. Kucharczyk,[27] V. Kudryavtsev,[36,w] A. K. Kuonen,[41] K. Kurek,[29] T. Kvaratskheliya,[32,40] D. Lacarrere,[40] G. Lafferty,[56] A. Lai,[16] D. Lambert,[52] G. Lanfranchi,[19] C. Langenbruch,[9] T. Latham,[50] C. Lazzeroni,[47] R. Le Gac,[6] J. van Leerdam,[43] J.-P. Lees,[4] A. Leflat,[33,40] J. Lefrançois,[7] R. Lefèvre,[5] F. Lemaitre,[40] E. Lemos Cid,[39] O. Leroy,[6] T. Lesiak,[27] B. Leverington,[12] Y. Li,[7] T. Likhomanenko,[35,67] R. Lindner,[40] C. Linn,[40] F. Lionetto,[42] B. Liu,[16] X. Liu,[3] D. Loh,[50] I. Longstaff,[53] J. H. Lopes,[2] D. Lucchesi,[23,o] M. Lucio Martinez,[39] H. Luo,[52] A. Lupato,[23] E. Luppi,[17,g] O. Lupton,[57] A. Lusiani,[24] X. Lyu,[63] F. Machefert,[7] F. Maciuc,[30] O. Maev,[31] K. Maguire,[56] S. Malde,[57] A. Malinin,[67] T. Maltsev,[36] G. Manca,[7] G. Mancinelli,[6] P. Manning,[61] J. Maratas,[5,v] J. F. Marchand,[4] U. Marconi,[15] C. Marin Benito,[38] P. Marino,[24,t] J. Marks,[12] G. Martellotti,[26] M. Martin,[6] M. Martinelli,[41] D. Martinez Santos,[39] F. Martinez Vidal,[68] D. Martins Tostes,[2] L. M. Massacrier,[7] A. Massafferri,[1] R. Matev,[40] A. Mathad,[50] Z. Mathe,[40] C. Matteuzzi,[21] A. Mauri,[42] B. Maurin,[41] A. Mazurov,[47] M. McCann,[55] J. McCarthy,[47] A. McNab,[56] R. McNulty,[13] B. Meadows,[59] F. Meier,[10] M. Meissner,[12] D. Melnychuk,[29] M. Merk,[43] A. Merli,[22,q] E. Michielin,[23] D. A. Milanes,[65] M.-N. Minard,[4] D. S. Mitzel,[12] A. Mogini,[8] J. Molina Rodriguez,[62] I. A. Monroy,[65] S. Monteil,[5] M. Morandin,[23] P. Morawski,[28] A. Mordà,[6] M. J. Morello,[24,t] J. Moron,[28] A. B. Morris,[52] R. Mountain,[61] F. Muheim,[52] M. Mulder,[43] M. Mussini,[15] D. Müller,[56] J. Müller,[10] K. Müller,[42] V. Müller,[10] P. Naik,[48] T. Nakada,[41] R. Nandakumar,[51] A. Nandi,[57] I. Nasteva,[2] M. Needham,[52] N. Neri,[22] S. Neubert,[12] N. Neufeld,[40] M. Neuner,[12] A. D. Nguyen,[41] C. Nguyen-Mau,[41,n] S. Nieswand,[9] R. Niet,[10] N. Nikitin,[33] T. Nikodem,[12] A. Novoselov,[37] D. P. O'Hanlon,[50] A. Oblakowska-Mucha,[28] V. Obraztsov,[37] S. Ogilvy,[19] R. Oldeman,[49] C. J. G. Onderwater,[69] J. M. Otalora Goicochea,[2] A. Otto,[40] P. Owen,[42] A. Oyanguren,[68] P. R. Pais,[41] A. Palano,[14,d] F. Palombo,[22,q] M. Palutan,[19] J. Panman,[40] A. Papanestis,[51] M. Pappagallo,[14,d] L. L. Pappalardo,[17,g] W. Parker,[60] C. Parkes,[56] G. Passaleva,[18] A. Pastore,[14,d] G. D. Patel,[54] M. Patel,[55] C. Patrignani,[15,e] A. Pearce,[56,51] A. Pellegrino,[43] G. Penso,[26] M. Pepe Altarelli,[40] S. Perazzini,[40] P. Perret,[5] L. Pescatore,[47] K. Petridis,[48] A. Petrolini,[20,h] A. Petrov,[67] M. Petruzzo,[22,q] E. Picatoste Olloqui,[38] B. Pietrzyk,[4] M. Pikies,[27] D. Pinci,[26] A. Pistone,[20] A. Piucci,[12] S. Playfer,[52] M. Plo Casasus,[39] T. Poikela,[40] F. Polci,[8] A. Poluektov,[50,36] I. Polyakov,[61] E. Polycarpo,[2] G. J. Pomery,[48] A. Popov,[37] D. Popov,[11,40] B. Popovici,[30] S. Poslavskii,[37] C. Potterat,[2] E. Price,[48] J. D. Price,[54] J. Prisciandaro,[39] A. Pritchard,[54] C. Prouve,[48] V. Pugatch,[46] A. Puig Navarro,[41] G. Punzi,[24,p] W. Qian,[57] R. Quagliani,[7,48] B. Rachwal,[27] J. H. Rademacker,[48] M. Rama,[24] M. Ramos Pernas,[39] M. S. Rangel,[2] I. Raniuk,[45] G. Raven,[44] F. Redi,[55] S. Reichert,[10] A. C. dos Reis,[1] C. Remon Alepuz,[68] V. Renaudin,[7] S. Ricciardi,[51] S. Richards,[48] M. Rihl,[40] K. Rinnert,[54] V. Rives Molina,[38] P. Robbe,[7,40] A. B. Rodrigues,[1] E. Rodrigues,[59] J. A. Rodriguez Lopez,[65] P. Rodriguez Perez,[56,†] A. Rogozhnikov,[35] S. Roiser,[40] A. Rollings,[57] V. Romanovskiy,[37] A. Romero Vidal,[39] J. W. Ronayne,[13] M. Rotondo,[19] M. S. Rudolph,[61] T. Ruf,[40] P. Ruiz Valls,[68] J. J. Saborido Silva,[39] E. Sadykhov,[32] N. Sagidova,[31] B. Saitta,[16,f] V. Salustino Guimaraes,[2] C. Sanchez Mayordomo,[68] B. Sanmartin Sedes,[39] R. Santacesaria,[26] C. Santamarina Rios,[39] M. Santimaria,[19] E. Santovetti,[25,j] A. Sarti,[19,k] C. Satriano,[26,s] A. Satta,[25] D. M. Saunders,[48] D. Savrina,[32,33] S. Schael,[9] M. Schellenberg,[10]

M. Schiller,[40] H. Schindler,[40] M. Schlupp,[10] M. Schmelling,[11] T. Schmelzer,[10] B. Schmidt,[40] O. Schneider,[41] A. Schopper,[40] K. Schubert,[10] M. Schubiger,[41] M.-H. Schune,[7] R. Schwemmer,[40] B. Sciascia,[19] A. Sciubba,[26,k] A. Semennikov,[32] A. Sergi,[47] N. Serra,[42] J. Serrano,[6] L. Sestini,[23] P. Seyfert,[21] M. Shapkin,[37] I. Shapoval,[45] Y. Shcheglov,[31] T. Shears,[54] L. Shekhtman,[36,w] V. Shevchenko,[67] A. Shires,[10] B. G. Siddi,[17,40] R. Silva Coutinho,[42] L. Silva de Oliveira,[2] G. Simi,[23,o] S. Simone,[14,d] M. Sirendi,[49] N. Skidmore,[48] T. Skwarnicki,[61] E. Smith,[55] I. T. Smith,[52] J. Smith,[49] M. Smith,[55] H. Snoek,[43] M. D. Sokoloff,[59] F. J. P. Soler,[53] B. Souza De Paula,[2] B. Spaan,[10] P. Spradlin,[53] S. Sridharan,[40] F. Stagni,[40] M. Stahl,[12] S. Stahl,[40] P. Stefko,[41] S. Stefkova,[55] O. Steinkamp,[42] S. Stemmle,[12] O. Stenyakin,[37] S. Stevenson,[57] S. Stoica,[30] S. Stone,[61] B. Storaci,[42] S. Stracka,[24,p] M. Straticiuc,[30] U. Straumann,[42] L. Sun,[59] W. Sutcliffe,[55] K. Swientek,[28] V. Syropoulos,[44] M. Szczekowski,[29] T. Szumlak,[28] S. T'Jampens,[4] A. Tayduganov,[6] T. Tekampe,[10] M. Teklishyn,[7] G. Tellarini,[17,g] F. Teubert,[40] E. Thomas,[40] J. van Tilburg,[43] M. J. Tilley,[55] V. Tisserand,[4] M. Tobin,[41] S. Tolk,[49] L. Tomassetti,[17,g] D. Tonelli,[40] S. Topp-Joergensen,[57] F. Toriello,[61] E. Tournefier,[4] S. Tourneur,[41] K. Trabelsi,[41] M. Traill,[53] M. T. Tran,[41] M. Tresch,[42] A. Trisovic,[40] A. Tsaregorodtsev,[6] P. Tsopelas,[43] A. Tully,[49] N. Tuning,[43] A. Ukleja,[29] A. Ustyuzhanin,[35] U. Uwer,[12] C. Vacca,[16,f] V. Vagnoni,[15,40] A. Valassi,[40] S. Valat,[40] G. Valenti,[15] A. Vallier,[7] R. Vazquez Gomez,[19] P. Vazquez Regueiro,[39] S. Vecchi,[17] M. van Veghel,[43] J. J. Velthuis,[48] M. Veltri,[18,r] G. Veneziano,[41] A. Venkateswaran,[61] M. Vernet,[5] M. Vesterinen,[12] B. Viaud,[7] D. Vieira,[1] M. Vieites Diaz,[39] X. Vilasis-Cardona,[38,m] V. Volkov,[33] A. Vollhardt,[42] B. Voneki,[40] A. Vorobyev,[31] V. Vorobyev,[36,w] C. Voß,[66] J. A. de Vries,[43] C. Vázquez Sierra,[39] R. Waldi,[66] C. Wallace,[50] R. Wallace,[13] J. Walsh,[24] J. Wang,[61] D. R. Ward,[49] H. M. Wark,[54] N. K. Watson,[47] D. Websdale,[55] A. Weiden,[42] M. Whitehead,[40] J. Wicht,[50] G. Wilkinson,[57,40] M. Wilkinson,[61] M. Williams,[40] M. P. Williams,[47] M. Williams,[58] T. Williams,[47] F. F. Wilson,[51] J. Wimberley,[60] J. Wishahi,[10] W. Wislicki,[29] M. Witek,[27] G. Wormser,[7] S. A. Wotton,[49] K. Wraight,[53] S. Wright,[49] K. Wyllie,[40] Y. Xie,[64] Z. Xing,[61] Z. Xu,[41] Z. Yang,[3] H. Yin,[64] J. Yu,[64] X. Yuan,[36,w] O. Yushchenko,[37] K. A. Zarebski,[47] M. Zavertyaev,[11,c] L. Zhang,[3] Y. Zhang,[7] A. Zhelezov,[12] Y. Zheng,[63] A. Zhokhov,[32] X. Zhu,[3] V. Zhukov,[9] and S. Zucchelli[15]

(LHCb Collaboration)

[1]*Centro Brasileiro de Pesquisas Físicas (CBPF), Rio de Janeiro, Brazil*
[2]*Universidade Federal do Rio de Janeiro (UFRJ), Rio de Janeiro, Brazil*
[3]*Center for High Energy Physics, Tsinghua University, Beijing, China*
[4]*LAPP, Université Savoie Mont-Blanc, CNRS/IN2P3, Annecy-Le-Vieux, France*
[5]*Clermont Université, Université Blaise Pascal, CNRS/IN2P3, LPC, Clermont-Ferrand, France*
[6]*CPPM, Aix-Marseille Université, CNRS/IN2P3, Marseille, France*
[7]*LAL, Université Paris-Sud, CNRS/IN2P3, Orsay, France*
[8]*LPNHE, Université Pierre et Marie Curie, Université Paris Diderot, CNRS/IN2P3, Paris, France*
[9]*I. Physikalisches Institut, RWTH Aachen University, Aachen, Germany*
[10]*Fakultät Physik, Technische Universität Dortmund, Dortmund, Germany*
[11]*Max-Planck-Institut für Kernphysik (MPIK), Heidelberg, Germany*
[12]*Physikalisches Institut, Ruprecht-Karls-Universität Heidelberg, Heidelberg, Germany*
[13]*School of Physics, University College Dublin, Dublin, Ireland*
[14]*Sezione INFN di Bari, Bari, Italy*
[15]*Sezione INFN di Bologna, Bologna, Italy*
[16]*Sezione INFN di Cagliari, Cagliari, Italy*
[17]*Sezione INFN di Ferrara, Ferrara, Italy*
[18]*Sezione INFN di Firenze, Firenze, Italy*
[19]*Laboratori Nazionali dell'INFN di Frascati, Frascati, Italy*
[20]*Sezione INFN di Genova, Genova, Italy*
[21]*Sezione INFN di Milano Bicocca, Milano, Italy*
[22]*Sezione INFN di Milano, Milano, Italy*
[23]*Sezione INFN di Padova, Padova, Italy*
[24]*Sezione INFN di Pisa, Pisa, Italy*
[25]*Sezione INFN di Roma Tor Vergata, Roma, Italy*
[26]*Sezione INFN di Roma La Sapienza, Roma, Italy*
[27]*Henryk Niewodniczanski Institute of Nuclear Physics Polish Academy of Sciences, Kraków, Poland*
[28]*AGH - University of Science and Technology, Faculty of Physics and Applied Computer Science, Kraków, Poland*
[29]*National Center for Nuclear Research (NCBJ), Warsaw, Poland*

[30]Horia Hulubei National Institute of Physics and Nuclear Engineering, Bucharest-Magurele, Romania
[31]Petersburg Nuclear Physics Institute (PNPI), Gatchina, Russia
[32]Institute of Theoretical and Experimental Physics (ITEP), Moscow, Russia
[33]Institute of Nuclear Physics, Moscow State University (SINP MSU), Moscow, Russia
[34]Institute for Nuclear Research of the Russian Academy of Sciences (INR RAN), Moscow, Russia
[35]Yandex School of Data Analysis, Moscow, Russia
[36]Budker Institute of Nuclear Physics (SB RAS), Novosibirsk, Russia
[37]Institute for High Energy Physics (IHEP), Protvino, Russia
[38]ICCUB, Universitat de Barcelona, Barcelona, Spain
[39]Universidad de Santiago de Compostela, Santiago de Compostela, Spain
[40]European Organization for Nuclear Research (CERN), Geneva, Switzerland
[41]Institute of Physics, Ecole Polytechnique Fédérale de Lausanne (EPFL), Lausanne, Switzerland
[42]Physik-Institut, Universität Zürich, Zürich, Switzerland
[43]Nikhef National Institute for Subatomic Physics, Amsterdam, Netherlands
[44]Nikhef National Institute for Subatomic Physics and VU University Amsterdam, Amsterdam, Netherlands
[45]NSC Kharkiv Institute of Physics and Technology (NSC KIPT), Kharkiv, Ukraine
[46]Institute for Nuclear Research of the National Academy of Sciences (KINR), Kyiv, Ukraine
[47]University of Birmingham, Birmingham, United Kingdom
[48]H.H. Wills Physics Laboratory, University of Bristol, Bristol, United Kingdom
[49]Cavendish Laboratory, University of Cambridge, Cambridge, United Kingdom
[50]Department of Physics, University of Warwick, Coventry, United Kingdom
[51]STFC Rutherford Appleton Laboratory, Didcot, United Kingdom
[52]School of Physics and Astronomy, University of Edinburgh, Edinburgh, United Kingdom
[53]School of Physics and Astronomy, University of Glasgow, Glasgow, United Kingdom
[54]Oliver Lodge Laboratory, University of Liverpool, Liverpool, United Kingdom
[55]Imperial College London, London, United Kingdom
[56]School of Physics and Astronomy, University of Manchester, Manchester, United Kingdom
[57]Department of Physics, University of Oxford, Oxford, United Kingdom
[58]Massachusetts Institute of Technology, Cambridge, Massachusetts, USA
[59]University of Cincinnati, Cincinnati, Ohio, USA
[60]University of Maryland, College Park, Maryland, USA
[61]Syracuse University, Syracuse, New York, USA
[62]Pontifícia Universidade Católica do Rio de Janeiro (PUC-Rio), Rio de Janeiro, Brazil
[associated with Universidade Federal do Rio de Janeiro (UFRJ), Rio de Janeiro, Brazil]
[63]University of Chinese Academy of Sciences, Beijing, China
(associated with Center for High Energy Physics, Tsinghua University, Beijing, China)
[64]Institute of Particle Physics, Central China Normal University, Wuhan, Hubei, China
(associated with Center for High Energy Physics, Tsinghua University, Beijing, China)
[65]Departamento de Fisica, Universidad Nacional de Colombia, Bogota, Colombia
(associated with LPNHE, Université Pierre et Marie Curie, Université Paris Diderot, CNRS/IN2P3, Paris, France)
[66]Institut für Physik, Universität Rostock, Rostock, Germany
(associated with Physikalisches Institut, Ruprecht-Karls-Universität Heidelberg, Heidelberg, Germany)
[67]National Research Centre Kurchatov Institute, Moscow, Russia
[associated with Institute of Theoretical and Experimental Physics (ITEP), Moscow, Russia]
[68]Instituto de Fisica Corpuscular, Centro Mixto Universidad de Valencia - CSIC, Valencia, Spain
(associated with ICCUB, Universitat de Barcelona, Barcelona, Spain)
[69]Van Swinderen Institute, University of Groningen, Groningen, Netherlands
(associated with Nikhef National Institute for Subatomic Physics, Amsterdam, Netherlands)

[†]Deceased.
[a]Universidade Federal do Triângulo Mineiro (UFTM), Uberaba-MG, Brazil.
[b]Laboratoire Leprince-Ringuet, Palaiseau, France.
[c]P.N. Lebedev Physical Institute, Russian Academy of Science (LPI RAS), Moscow, Russia.
[d]Università di Bari, Bari, Italy.
[e]Università di Bologna, Bologna, Italy.
[f]Università di Cagliari, Cagliari, Italy.
[g]Università di Ferrara, Ferrara, Italy.
[h]Università di Genova, Genova, Italy.
[i]Università di Milano Bicocca, Milano, Italy.
[j]Università di Roma Tor Vergata, Roma, Italy.

[k]Università di Roma La Sapienza, Roma, Italy.
[l]AGH - University of Science and Technology, Faculty of Computer Science, Electronics and Telecommunications, Kraków, Poland.
[m]LIFAELS, La Salle, Universitat Ramon Llull, Barcelona, Spain.
[n]Hanoi University of Science, Hanoi, Viet Nam.
[o]Università di Padova, Padova, Italy.
[p]Università di Pisa, Pisa, Italy.
[q]Università degli Studi di Milano, Milano, Italy.
[r]Università di Urbino, Urbino, Italy.
[s]Università della Basilicata, Potenza, Italy.
[t]Scuola Normale Superiore, Pisa, Italy.
[u]Università di Modena e Reggio Emilia, Modena, Italy.
[v]Iligan Institute of Technology (IIT), Iligan, Philippines.
[w]Novosibirsk State University, Novosibirsk, Russia.